## EDGE ARTICLE

# Tandem mechanochemical engineering yields highly crystalline metal–organic frameworks

Zhuorigebatu Tegudeer [ID] and Wen-Yang Gao [ID] *

The formation of highly crystalline metal–organic frameworks (MOFs) relies on reversible metal–ligand (M–L) bond formation under conditions that enable defect annealing. While solvothermal synthesis remains the most common method for producing crystalline MOFs, mechanochemical synthesis is emerging as a greener alternative. However, the solid-state nature of mechanochemical reactions—even when assisted by catalytic amounts of liquid additives—limits molecular mobility, thereby impeding defect annealing and crystallization. This work introduces a tandem mechanochemical engineering strategy to achieve highly crystalline MOFs by incorporating a second class of reversible bond formation—imine condensation—alongside traditional M–L coordination. The critical role of cooperative dynamics between M–L and imine reversible bonds is highlighted by systematic investigations using similar high-connectivity ligand analogues featuring irreversible covalent linkages (e.g., ether, amide, or alkyne), which fail to produce quality crystalline MOF phases under mechanochemical conditions. The synergistic effect of dual reversible bonds addresses sluggish reaction kinetics inherent to solid-state processes, enhances crystallization kinetics, and enables the efficient mechanochemical synthesis of MOFs with improved crystallinity under ambient conditions, particularly for frameworks constructed from high-connectivity ligands.
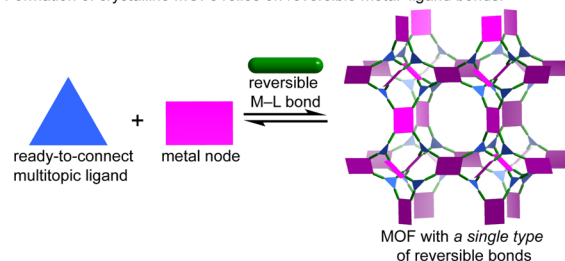
## Introduction

The formation of highly crystalline metal–organic frameworks (MOFs) hinges on reversible metal–ligand (M–L) dative bond formation between ready-to-connect organic ligands and metal ions under appropriate synthetic conditions (Fig. 1a).[1–4] Traditionally, solvothermal methods dominate MOF synthesis, where reactants are dissolved in excess organic solvents and incubated at elevated temperatures over extended periods.[5–7] These conditions allow the system to reach thermodynamic equilibrium, enabling defect annealing and promoting the growth of well-ordered crystalline phases.

As a more sustainable alternative, mechanochemical synthesis has emerged, using mechanical energy to drive MOF assembly under solvent-free conditions or in the presence of only catalytic amounts of solvents.[8–19] However, the (near) solid-state nature of mechanochemistry limits molecular mobility and typically reduces the reversibility of M–L bonds. Our previous studies have shown that ligand exchange kinetics significantly impact the crystallinity of mechanochemically synthesized MOFs, and that relatively inert metals, coupled with low M–L bond reversibility, often yield only small crystallites.[20,21] This constraint—the decreased reversibility of M–L bonds under solid-state conditions—poses a particular
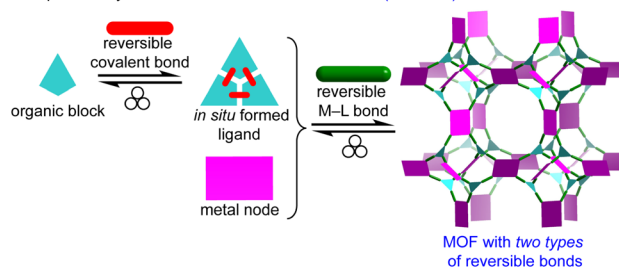


Fig. 1 (a) Conventional MOF synthesis typically relies on a single type of reversible dative bonds between metal ions and organic ligands. This reversibility enables defect annealing and facilitates the formation of crystalline MOFs. (b) This work introduces a synthetic strategy that incorporates reversible covalent bonds alongside the M–L dative bonds during mechanochemical MOF synthesis. The synergy between these two types of reversible interactions is expected to enhance the crystallinity of MOFs prepared via mechanochemistry.

Department of Chemistry and Biochemistry, Nanoscale & Quantum Phenomena Institute, Ohio University, Athens, Ohio 45701, USA. E-mail: gaow@ohio.edu

challenge for incorporating bulky or inherently sluggish ligands that require dynamic chemical environments to assemble into ordered MOF structures. This explains why multitopic ligands with 2 to 4 connection points have been mechanochemically integrated into MOFs,[22–40] but ligands with higher connectivity are rarely encountered in mechanochemistry.[41] Herein, we propose tandem mechanochemical engineering as a new synthetic strategy to overcome this challenge and enable the efficient incorporation of bulky or less mobile ligands (*e.g.*, high-connectivity multitopic ligands) into MOFs under mechanochemical conditions (Fig. 1b). Our earlier study showed that imines can be directly introduced into MOFs by mechanochemistry.[42] In contrast, the present work departs from that approach to tackle the sluggish reaction kinetics inherent to solid-state processes during crystalline phase formation. By introducing a second type of reversible bonds, namely a dynamic covalent imine bond, alongside the M–L dative bond, this tandem approach enables the one-pot mechanochemical synthesis of highly crystalline MOFs from high-connectivity

ligands. Remarkably, it also reduces reaction time by approximately 100-fold (*e.g.*, from typical 1.5 hours to 56 seconds or less). The use of multiple reversible interactions mitigates the limited molecular mobility inherent to solventless conditions and significantly expands the scope of mechanochemical synthesis to a broader family of MOFs with diverse topologies.

As a proof-of-concept, we selected **rht**-topology MOFs (Fig. 2a), which are typically constructed from highly connected hexacarboxylic ligands and metal paddlewheel dimers (*e.g.*, $Cu_2(OOC)_4$).[43–50] The (3,24)-connected **rht**-topology network represents a canonical example of reticular chemistry, employing supermolecular building blocks—specifically, 24-connected cuboctahedra composed of 24 isophthalate moieties and 12 dinuclear copper paddlewheel units.[51] These frameworks exemplify best practices in MOF reticular design, achieving record-high surface areas and free pore volumes through ligand expansion while avoiding framework interpenetration.[52–54] However, to the best of our knowledge, no **rht**-topology MOFs has been synthesized mechanochemically. While the fast kinetics of Cu–O bond formation have enabled the mechanochemical assembly of copper paddlewheel-based MOFs[26,29,55,56] (*e.g.*, HKUST-1,[57] MOF-14,[58] and MOF-505 (ref. 59)) using tricarboxylic or tetracarboxylic ligands, the incorporation of hexacarboxylic ligands remain a significant challenge under mechanochemical conditions. This difficulty is tentatively attributed to the high lattice energy barrier that must be overcome during the annealing of M–L defects involving metal nodes and high-connectivity ligands.

## Results and discussion

Two hexacarboxylic ligands featuring ether and amide linkages (Fig. 2b)—both previously known to yield **rht**-topology MOFs *via* solvothermal synthesis[47,60,61]—were extensively attempted for mechanochemical assembly under various milling conditions. However, powder X-ray diffraction (PXRD, Table S1 and Fig. 3a and S1) reveal poorly crystalline phases for the ether-linked ligand. The amide-linked ligand produced relatively broad PXRD patterns matching the calculated **rht** structure under certain conditions (Table S2 and Fig. 3a and S2). Nevertheless, $N_2$ adsorption isotherms at 77 K (Fig. S3) showed significantly reduced Brunauer–Emmett–Teller (BET) surface areas compared to those obtained from solvothermal synthesis (215–1069 $m^2$ $g^{-1}$ *vs.* 3160 $m^2$ $g^{-1}$).[61] The parameter scope of our mechanochemical trials included variation in the type and amount of liquid additive (*e.g.*, *N*,*N*-dimethylformamide, DMF), milling time, and milling frequency. Moreover, we also tested high-temperature ball-milling conditions[62]—blowing 80 °C and 120 °C hot air onto the stainless-steel milling jars–for reactions involving both the amide- and ether-linked ligands, in order to evaluate how elevated temperature influences reagent mobility in the solid state and the resulting crystallinity during the MOF assembly. However, no improvement in the PXRD patterns (Fig. S4) was observed, and reflections corresponding to elemental Cu appeared instead. These unsuccessful attempts underscore the challenge of incorporating high-connectivity ligands into crystalline MOFs under mechanochemical
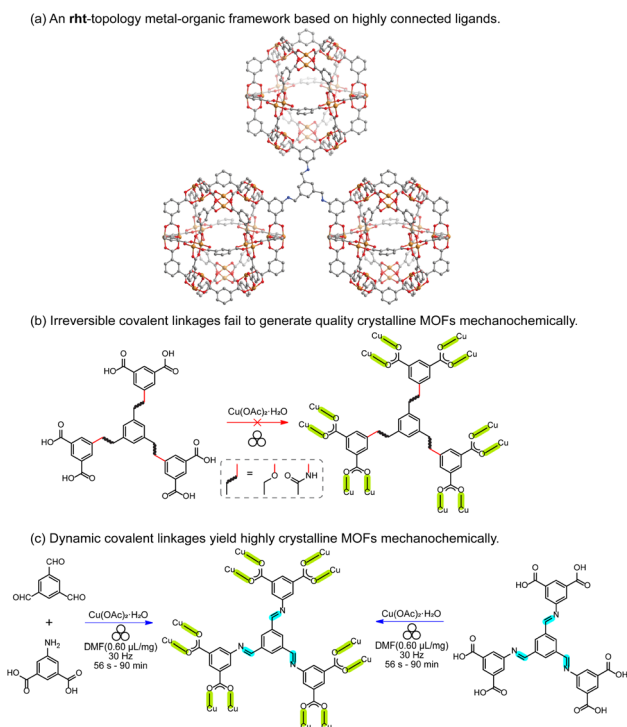


**Fig. 2** (a) An example of the **rht**-topology MOF is composed of hexacarboxylic ligands and metal paddlewheel dimers. This network can be simplified into 3-connected organic nodes and 24-connected cuboctahedra composed of 24 isophthalate moieties and 12 dinuclear copper paddlewheel units. (b) Two hexacarboxylic ligands featuring ether and amide linkages—both known to yield **rht**-topology MOFs *via* solvothermal synthesis—were extensively tested under various mechanochemical milling conditions, but failed to produce high-quality crystalline MOFs. (c) Incorporating reversible covalent linkages (*e.g.*, imine) into highly connected ligands mitigates the irreversibility of M–L interactions by effectively reducing ligand connectivity. This strategy enables the successful formation of a highly crystalline **rht**-topology MOF, either through a one-pot cascade reaction or by using a pre-synthesized imine-based hexacarboxylic ligand. All the reversible bonds, including Cu–O and imine linkages, are highlighted.
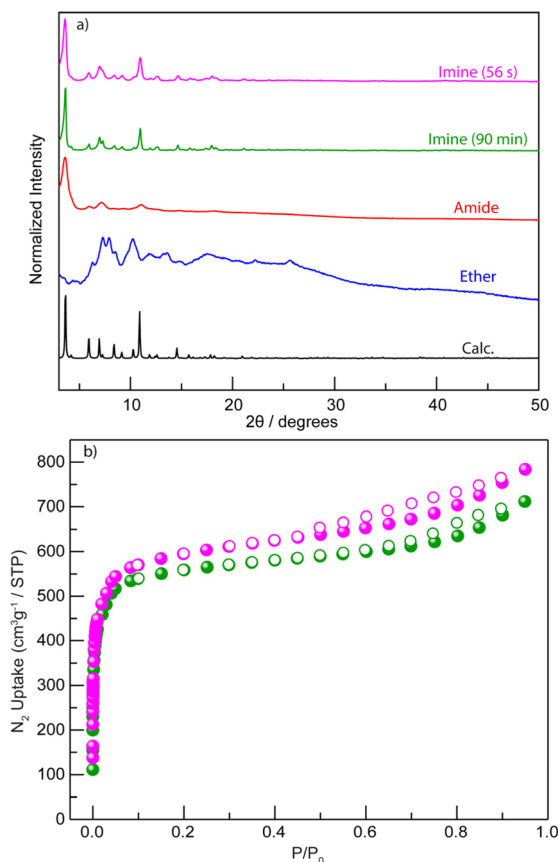
Fig. 3 (a) PXRD patterns of mechanochemically obtained solids derived from ether- (blue), amide- (red), imine-linked ligands (90 min, green and 56 s, magenta) are compared to the calculated pattern for the amide-linked MOF (black). (b) $N_2$ adsorption isotherms at 77 K were collected for imine-based **rht**-topology MOFs prepared mechanochemically (90 min, green dot; 56 s, magenta dot).

conditions, likely due to the reduced reversibility of M–L bond formation in the (near) solid environment and other potential deleterious reactions observed for Cu(II).

In contrast to the previously tested irreversible covalent linkages (*e.g.*, ether and amide), we propose that incorporating reversible or dynamic covalent linkage (*e.g.*, imine) into highly connected ligands can mitigate the irreversibility of M–L interactions by effectively reducing the number of ligand connectivity during the assembly process (Fig. 2c). This enhanced reversibility is expected to facilitate the mechanochemical crystallization of MOFs from otherwise sluggish, highly connected ligands. Therefore, we initiated the mechanochemical synthesis of an **rht**-topology MOF by milling trimesaldehyde, 5-aminoisophthalic acid, and Cu(OAc)$_2$·H$_2$O in a molar ratio of 1 : 3 : 3 in the presence of DMF ($\eta = 0.60$ μL mg$^{-1}$, Table S3 and Fig. S5) using a stainless-steel milling cup and two stainless steel balls. The reaction mixture was milled at 30 Hz for 90 min. The resultant blue solids were washed with acetone and collected by centrifugation. PXRD analysis (Fig. 3a) confirmed the phase purity of the obtained imine-derived **rht**-topolgy MOF, based on the excellent agreement between the experimental patterns and the simulated ones (calculated from

the amide-linked framework). Additionally, we synthesized the imine-based hexacarboxylic ligand under standard solution-phase condensation conditions catalyzed by acetic acid (see details in SI) and used it for the mechanochemical synthesis of the above **rht**-MOF. The isolated imine ligand was confirmed by ${}^1$H NMR (Fig. S6), high-resolution mass spectrometry (HRMS), and infrared spectroscopy (Fig. S7). The mechanochemical MOF product obtained from this pre-synthesized imine ligand was identified by PXRD (Fig. S8) as the same phase as the **rht**-MOF prepared *via* the one-pot cascade reaction. This observation is consistent with previous findings that mechanochemical synthesis can deliver crystalline imine-based covalent organic frameworks[63–67] and MOFs,[42] and further demonstrates the imine formation and cleavage remain reversible under the applied mechanochemical conditions. In contrast, similar mechanochemical reactions employing the hexacarboxylic ligands with irreversible covalent ether or amide linkages failed to yield the targeted high-quality crystalline MOFs. This comparison underscores the effectiveness of our tandem mechanochemical engineering strategy, where the introduction of an additional class of reversible bonds significantly improves the crystallization of MOFs under mechanochemical conditions.

Moreover, due to the hydrolytic instability of the imine motif,[68,69] imine-based complexes and MOFs are well-suited for direct mechanochemical synthesis from aldehyde and primary amine precursors, along with the metal source.[42,70–72] We attempted a series of solvothermal reactions using the pre-synthesized imine-based hexacarboxylic acid ligand (see details in SI, Table S4, and Fig. S9) to access this **rht**-MOF. However, the yields were very low, or the reactions were unsuccessful. Consistent with the lability of the imine linkages, HRMS analysis of reaction solutions indicated that the ligand decomposed back into its aldehyde and amine precursors, particularly in water-rich environment. In contrast, the tandem mechanochemical approach not only avoids the decomposition pathways that often occur under solvothermal conditions, but also enables the formation of the first imine-based **rht**-MOF among its various analogues, eliminating the need for the tedious pre-synthesis of imine ligands.

Additional characterizations of the imine-based **rht**-MOF obtained by tandem mechanochemical synthesis include IR spectroscopy, thermogravimetric analysis (TGA), and $N_2$ adsorption analysis at 77 K. The IR spectrum (Fig. S10) shows that a strong peak emerged at 1371 cm$^{-1}$, attributed to the coordinated C=O stretch, validating the formation of the desired MOF. The TGA analysis (Fig. S11) reveals that the obtained imine-based **rht**-topology MOF exhibits thermal stability comparable to other known **rht**-MOFs,[60,61] which is stable up to 280 °C or above. Thus, the imine-based **rht**-MOF was activated by heating at 60 °C under high vacuum for 18 h prior to gas adsorption measurements. The permanent porosity of the imine-based **rht**-MOF was characterized by $N_2$ adsorption isotherms at 77 K (Fig. 3b), which provided a BET surface area of 2238 m$^2$ g$^{-1}$ ($P/P_0 = 0.007$–$0.03$). This value is somewhat lower than that of its amide analogue (3160 m$^2$ g$^{-1}$), likely due to the entrapment of molecular fragments from incomplete reactions

within the cavities, which partially occupy the pore volume. Nevertheless, the BET surface area of the mechanochemically synthesized imine-based **rht**-MOF remains higher than that of the solvothermally obtained samples (Fig. S12), which exhibit BET surface area values ranging from 1244 to 1265 $m^2 g^{-1}$ under the same activation conditions.

Furthermore, to evaluate how the second type of reversible bond influences reaction time, we systematically examined the minimum milling duration required to synthesize the imine-based **rht**-MOF (Table S5). Whereas many mechanochemical studies employ ~90 minutes milling times, well-defined PXRD patterns were observed in as little as 56 seconds (Fig. 3a), with all precursor-related PXRD peaks disappearing (Fig. S13). Remarkably, even after only 28 seconds, the MOF phase already dominates, with no apparent signatures of precursors. This rapid reaction yields materials of comparable quality to those produced at 90 min, as confirmed by $N_2$ adsorption isotherms at 77 K (Fig. 3b). The BET surface area calculated from the 56 seconds product is 2278 $m^2 g^{-1}$ ($P/P_0 = 0.007–0.03$), even slightly higher than that of the 90 min sample. This remarkably short reaction time highlights the critical role of dynamic imine bond in facilitating rapid MOF crystallization under mechanochemical conditions.

Tandem mechanochemical engineering also enables us to synthesize an expanded analogue of the imine-based **rht**-MOF by replacing trimesaldehyde with 1,3,5-tris(4-formylphenyl) benzene under similar milling conditions. The obtained dark green-colored crystalline solids were explored (Table S6; Fig. S14) and confirmed by PXRD (Fig. 4), consistent with the pattern calculated from an amide-linked MOF analogue.[73] The reaction progress was monitored by IR spectroscopy (Fig. S15), illustrating the appearance of coordinated carbonyl stretch at 1372 $cm^{-1}$. TGA (Fig. S16) and $N_2$ adsorption measurements (Fig. S17) provide additional characterization data on the mechanochemically obtained expanded **rht**-topology MOF. $N_2$ adsorption isotherms at 77 K, which provided a calculated BET

surface area of 976 $m^2 g^{-1}$ ($P/P_0 = 0.007–0.03$). The decreased surface area value of the mechanochemically obtained large-pore MOF compared to that of the calculated one remains common,[21,29,55] tentatively due to molecular fragments trapped in the expanded cavities. Control experiments to synthesize this expanded imine-linked **rht**-MOF under mechanochemical and solvothermal using the preformed imine-based expanded hexacarboxylic ligand were also attempted (Fig. S18–S21 and Table S7), which are consistent with observations in the last study.

In addition to the **rht**-topology MOFs, we also applied tandem mechanochemical engineering to an imine-based **pto**-topology MOF (Fig. 5a), isostructural to MOF-14.[58] Its direct mechanochemical synthesis was achieved by milling tri-mesaldehyde, 4-aminobenzoic acid, and $Cu(OAc)_2 \cdot H_2O$ in a molar ratio of 2 : 6 : 3 with the addition of DMF ($\eta = 0.90$ μL $mg^{-1}$, Fig. S22) for 60 min (Fig. S23 and Table S8). The harvested blue solids were characterized by a suite of solid-state characterizations, including PXRD, IR, TGA, and $N_2$ adsorption analysis. The PXRD pattern (Fig. 5a) matches well with that of an amide-based **pto**-MOF indicating an isostructural lattice. The IR spectrum (Fig. S24) confirms the coordinated C=O stretch observed at 1400 $cm^{-1}$ in the imine-linked **pto**-MOF illustrates the formation of dative bonds. In addition, the disappearance of



Fig. 5 (a) The PXRD pattern of mechanochemically obtained solids derived from the imine-linked ligand (red line) is compared to the calculated pattern from the amide-linked **pto**-topolgy MOF (black line). (b) $N_2$ adsorption isotherms at 77 K were collected for the imine-based **pto**-topolgy MOF prepared mechanochemically.
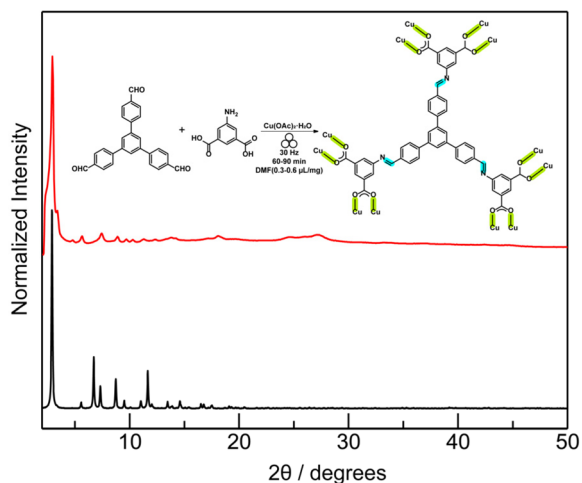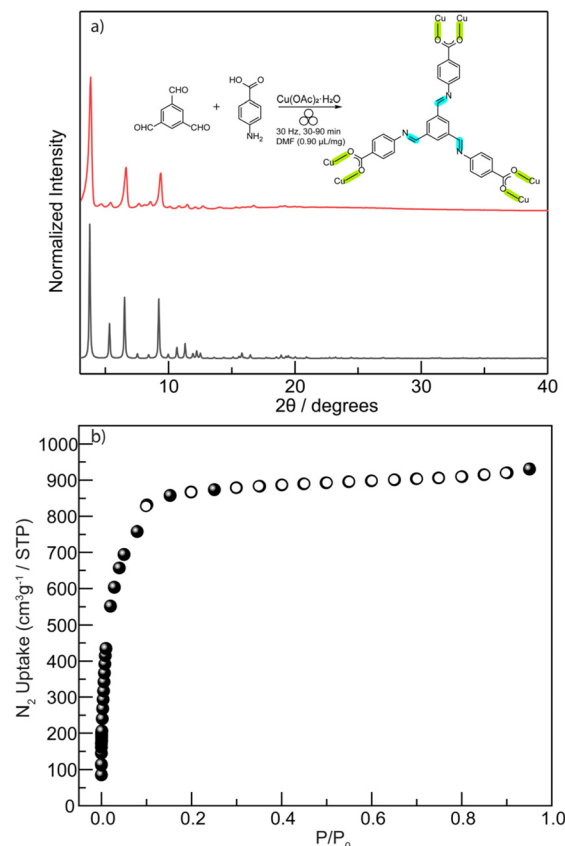


Fig. 4 An expanded **rht**-topology MOF featuring the imine-linkage allows for mechanochemical synthesis, confirmed by PXRD patterns (red line, as-synthesized; black line, calculated from the amide-linked isostructural MOF).

N–H stretches between 3473 cm$^{-1}$ and 3364 cm$^{-1}$ from the primary amine precursor highlights its conversion to imine bonds. The TGA plot (Fig. S25) shows its thermal stability until 280 °C, comparable to the previous imine-based **rht**-MOF. Notably, while this imine-based **pto**-MOF can be synthesized mechanochemically using the preformed imine-based tricarboxylic ligand (Fig. S26–28), direct solvothermal synthesis fails (see details in SI and Table S9), largely due to the ready collapse of the imine ligand.

Though MOF-14 allows for its direct mechanochemical synthesis using 1,3,5-tris(4-carboxylphenyl)benzene (H$_3$btb) and Cu(OAc)$_2$·H$_2$O,[29,55] we have attempted a number of milling conditions using other extended tricarboxylic ligands featuring irreversible covalent linkages (*e.g.*, amide and alkyne) and not been able to generate any crystalline MOF phases (Tables S10–S11 and Fig. S29–S32). This is another highlight that tandem mechanochemical engineering streamlines the incorporation of bulky or sluggish ligands into MOFs. In addition, the solvothermally obtained MOF-14 analogues with the amide[74,75] and alkyne[76–79] linkages readily collapse upon solvent removal (even activated by supercritical CO$_2$) and thus were not characterized by N$_2$ adsorption analysis in the literature. In contrast, our mechanochemically built imine-based **pto**-MOF still demonstrates its permanent high porosity based on N$_2$ adsorption analysis at 77 K (Fig. 5b). The BET surface area was calculated to be 3136 m$^2$ g$^{-1}$ ($P/P_0$ = 0.007–0.03), representing the highest value reported to date for mechanochemically prepared porous materials.

The developed tandem mechanochemical engineering approach integrates two types of reversible bond formation processes into one single mechanochemical step, provides an alternative to bypass high lattice energy associated with multitopic ligands required to anneal defects, and incorporates hydrolytically unstable imine motifs into extended MOFs. The introduction of reversible dynamic covalent bonds coupled with the reversible M–L bond overcomes the sluggish reaction kinetics typically associated with solid-state reactions and expands the applicability of mechanochemical MOF synthesis.

The byproduct of the reaction between carboxylic ligands and copper acetate is acetic acid, which is a known catalyst for imine condensation. Thus, the dative bond formation releases acetic acid, which accelerates the kinetics of imine bond formation and breakage. This process creates an autocatalytic cycle that promotes defect annealing and ultimately yields high-quality crystalline MOF phases. Fig. 6 presents a schematic energy diagram comparing the developed tandem mechanochemical engineering with traditional solvothermal methods. Incorporating high-connectivity ligands into crystalline MOF lattices typically requires high activation energy during crystal nucleation and growth, which is usually achievable only under solvothermal conditions. In contrast, introducing a second type of reversible bond in the mechanochemical synthesis segments the otherwise high activation barrier for bulky ligand assembly into a series of imine-mediated steps with lower individual barriers. This stepwise alternative pathway facilitates smoother kinetic transitions, accelerates crystallization, promotes defect annealing, and eventually drives the system toward the thermodynamically favored crystalline phases.

## Conclusions

In conclusion, we report a powerful synthetic strategy—tandem mechanochemical engineering—to access MOFs that are challenging under conventional mechanochemical conditions. The incorporation of a second type of reversible dynamic bonds (*e.g.*, imine) coupled with the M–L dative bonds yields highly crystalline MOFs in solid-state reactions, which also decreases reaction time to as little as 56 seconds. The synergy of M–L and imine reversible bonds promotes crystallization kinetics and facilitates efficient mechanochemical synthesis of MOFs with improved crystallinity under ambient conditions, especially those based on high-connectivity ligands. This strategy offers a general and efficient pathway for constructing well-ordered frameworks *via* solvent-free routes, while streamlining *in situ* ligand synthesis and MOF formation in a one-pot process.

## Author contributions

WG and ZT conceived and designed the project. ZT carried out the materials synthesis and characterization as well as performed data analysis. Both authors discussed the results and wrote the manuscript.

## Conflicts of interest

The authors declare the following competing financial interest(s): a provisional patent application has been filed based on the results reported in this manuscript. This patent application is held by Ohio University. The authors have no other relevant financial interests to disclose.

## Data availability

The data supporting this article have been included as part of the supplementary information (SI). Supplementary
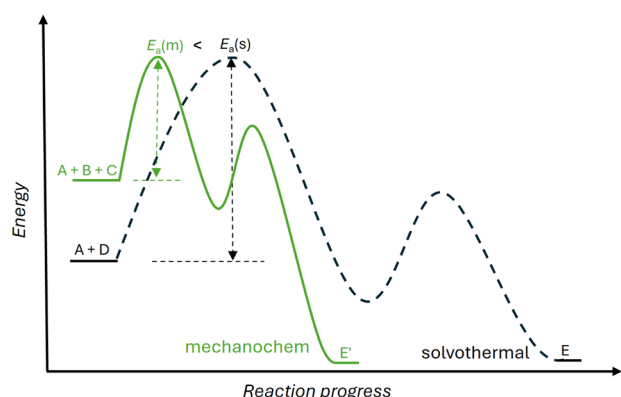


**Fig. 6** A schematic energy diagram comparing tandem mechanochemical engineering and solvothermal methods for crystal nucleation and growth steps. The tandem mechanochemical approach provides an alternative reaction pathway with reduced activation energies (green solid line), in contrast to the solvothermal method (black dash line) required for incorporating high-connectivity ligands.

## Acknowledgements

## References

1 J. Han, X. He, J. Liu, R. Ming, M. Lin, H. Li, X. Zhou and H. Deng, Determining factors in the growth of MOF single crystals unveiled by *in situ* interface imaging, *Chem*, 2022, **8**, 1637–1657.

2 A. A. Ezazi, W.-Y. Gao and D. C. Powers, Leveraging Exchange Kinetics for the Synthesis of Atomically Precise Porous Catalysts, *ChemCatChem*, 2021, **13**, 2117–2131.

3 W. Lu, Z. Wei, Z.-Y. Gu, T.-F. Liu, J. Park, J. Park, J. Tian, M. Zhang, Q. Zhang, T. Gentle Iii, M. Bosch and H.-C. Zhou, Tuning the structure and function of metal–organic frameworks *via* linker design, *Chem. Soc. Rev.*, 2014, **43**, 5561–5593.

4 H. Ghasempour, K.-Y. Wang, J. A. Powell, F. ZareKarizi, X.-L. Lv, A. Morsali and H.-C. Zhou, Metal–organic frameworks based on multicarboxylate linkers, *Coord. Chem. Rev.*, 2021, **426**, 213542.

5 N. Stock and S. Biswas, Synthesis of metal-organic frameworks (MOFs): routes to various MOF topologies, morphologies, and composites, *Chem. Rev.*, 2012, **112**, 933–969.

6 M. Safaei, M. M. Foroughi, N. Ebrahimpoor, S. Jahani, A. Omidi and M. Khatami, A review on metal-organic frameworks: Synthesis and applications, *Trends Anal. Chem.*, 2019, **118**, 401–425.

7 V. F. Yusuf, N. I. Malek and S. K. Kailasa, Review on Metal-Organic Framework Classification, Synthetic Approaches, and Influencing Factors: Applications in Energy, Drug Delivery, and Wastewater Treatment, *ACS Omega*, 2022, **7**, 44507–44531.

8 J. M. Marrett, F. Effaty, X. Ottenwaelder and T. Friščić, Mechanochemistry for Metal-Organic Frameworks and Covalent-Organic Frameworks (MOFs, COFs): Methods, Materials, and Mechanisms, *Adv. Mater.*, 2025, 2418707.

9 T. Stolar, L. Batzdorf, S. Lukin, D. Žilić, C. Motillo, T. Friščić, F. Emmerling, I. Halasz and K. Užarević, In Situ Monitoring of the Mechanosynthesis of the Archetypal Metal-Organic Framework HKUST-1: Effect of Liquid Additives on the Milling Reactivity, *Inorg. Chem.*, 2017, **56**, 6599–6608.

10 T. Plant-Collins, Z. Tegudeer, D. V. Athapaththu, H. Ringle, J. Chen and W.-Y. Gao, Beyond Solution Chemistry: Mechanochemistry Enables Clustered Defects in Metal–Organic Frameworks, *Inorg. Chem.*, 2025, **64**, 17436–17447.

11 T. Stolar and K. Užarević, Mechanochemistry: an efficient and versatile toolbox for synthesis, transformation, and functionalization of porous metal-organic frameworks, *CrystEngComm*, 2020, **22**, 4511–4525.

12 D. Chen, J. Zhao, P. Zhang and S. Dai, Mechanochemical synthesis of metal–organic frameworks, *Polyhedron*, 2019, **162**, 59–64.

13 T. Friščić, C. Mottillo and H. M. Titi, Mechanochemistry for Synthesis, *Angew. Chem., Int. Ed.*, 2020, **59**(3), 1018–1029.

14 F. Afshariazar and A. Morsali, The unique opportunities of mechanosynthesis in green and scalable fabrication of metal–organic frameworks, *J. Mater. Chem. A*, 2022, **10**, 15332–15369.

15 C.-A. Tao and J.-F. Wang, Synthesis of Metal Organic Frameworks by Ball-Milling, *Crystals*, 2020, **11**, 15.

16 H. M. Titi, J.-L. Do, A. J. Howarth, K. Nagapudi and T. Friščić, Simple, scalable mechanosynthesis of metal-organic frameworks using liquid-assisted resonant acoustic mixing (LA-RAM), *Chem. Sci.*, 2020, **11**, 7578–7584.

17 O. Barreda, G. R. Lorzing and E. D. Bloch, Mechanochemical synthesis of two-dimensional metal-organic frameworks, *Powder Diffr.*, 2019, **34**, 119–123.

18 S. Głowniak, B. Szczęśniak, J. Choma and M. Jaroniec, Mechanochemistry: Toward green synthesis of metal–organic frameworks, *Mater. Today*, 2021, **46**, 109–124.

19 O. Barreda, G. A. Taggart, C. A. Rowland, G. P. A. Yap and E. D. Bloch, Mechanochemical Synthesis of Porous Molecular Assemblies, *Chem. Mater.*, 2018, **30**, 3975–3978.

20 F. E. Salvador, Z. Tegudeer, H. Locke and W.-Y. Gao, Facile mechanochemical synthesis of MIL-53 and its isoreticular analogues with a glance at reaction reversibility, *Dalton Trans.*, 2024, **53**, 4406–4411.

21 Z. Tegudeer, J. Moon, J. Wright, M. Das, G. Rubasinghege, W. Xu and W.-Y. Gao, Generic and facile mechanochemical access to versatile lattice-confined Pd(II)-based heterometallic sites, *Chem. Sci.*, 2024, **15**, 10126–10134.

22 A. Pichon, A. Lazuen-Garay and S. L. James, Solvent-free synthesis of a microporous metal-organic framework, *CrystEngComm*, 2006, **8**, 211–214.

23 Z. Wang, Z. Li, M. Ng and P. J. Milner, Rapid mechanochemical synthesis of metal–organic frameworks using exogenous organic base, *Dalton Trans.*, 2020, **49**, 16238–16244.

24 E. Y. Chen, R. M. Mandel and P. J. Milner, Evaluating solvothermal and mechanochemical routes towards the metal–organic framework $Mg_2$(m-dobdc), *CrystEngComm*, 2022, **24**, 7292–7297.

25 W. Yuan, J. O'Connor and S. L. James, Mechanochemical synthesis of homo- and hetero-rare-earth(iii) metal–organic frameworks by ball milling, *CrystEngComm*, 2010, **12**, 3515–3517.

26 W. Yuan, A. L. Garay, A. Pichon, R. Clowes, C. D. Wood, A. I. Cooper and S. L. James, Study of the mechanochemical formation and resulting properties of an archetypal MOF: $Cu_3(BTC)_2$ (BTC = 1,3,5-benzenetricarboxylate), *CrystEngComm*, 2010, **12**, 4063–4065.

27 P. J. Beldon, L. Fábián, R. S. Stein, A. Thirumurugan, A. K. Cheetham and T. Friščić, Rapid room-temperature synthesis of zeolitic imidazolate frameworks by using mechanochemistry, *Angew. Chem., Int. Ed.*, 2010, **49**, 9640–9643.

28 T. Friščić and L. Fábián, Mechanochemical conversion of a metal oxide into coordination polymers and porous frameworks using liquid-assisted grinding (LAG), *CrystEngComm*, 2009, **11**, 743–745.

29 M. Klimakow, P. Klobes, A. F. Thünemann, K. Rademann and F. Emmerling, Mechanochemical Synthesis of Metal−Organic Frameworks: A Fast and Facile Approach toward Quantitative Yields and High Specific Surface Areas, *Chem. Mater.*, 2010, **22**, 5216–5221.

30 B. Karadeniz, D. Žilić, I. Huskić, L. S. Germann, A. M. Fidelli, S. Muratović, I. Lončarić, M. Etter, R. E. Dinnebier, D. Barišić, N. Cindro, T. Islamoglu, O. K. Farha, T. Friščić and K. Užarević, Controlling the Polymorphism and Topology Transformation in Porphyrinic Zirconium Metal-Organic Frameworks *via* Mechanochemistry, *J. Am. Chem. Soc.*, 2019, **141**, 19214–19220.

31 B. Karadeniz, A. J. Howarth, T. Stolar, T. Islamoglu, I. Dejanović, M. Tireli, M. C. Wasson, S.-Y. Moon, O. K. Farha, T. Friščić and K. Užarević, Benign by Design: Green and Scalable Synthesis of Zirconium UiO-Metal–Organic Frameworks by Water-Assisted Mechanochemistry, *ACS Sustain. Chem. Eng.*, 2018, **6**, 15841–15849.

32 S. Darwish, S.-Q. Wang, D. M. Croker, G. M. Walker and M. J. Zaworotko, Comparison of Mechanochemistry *vs.* Solution Methods for Synthesis of 4,4′-Bipyridine-Based Coordination Polymers, *ACS Sustain. Chem. Eng.*, 2019, **7**, 19505–19512.

33 K. Užarević, T. C. Wang, S.-Y. Moon, A. M. Fidelli, J. T. Hupp, O. K. Farha and T. Friščić, Mechanochemical and solvent-free assembly of zirconium-based metal-organic frameworks, *Chem. Commun.*, 2016, **52**, 2133–2136.

34 D. Prochowicz, K. Sokołowski, I. Justyniak, A. Kornowicz, D. Fairen-Jimenez, T. Friščić and J. Lewiński, A mechanochemical strategy for IRMOF assembly based on pre-designed oxo-zinc precursors, *Chem. Commun.*, 2015, **51**, 4032–4035.

35 Y. Chen, J. Xiao, D. Lv, T. Huang, F. Xu, X. Sun, H. Xi, Q. Xia and Z. Li, Highly efficient mechanochemical synthesis of an indium based metal-organic framework with excellent water stability, *Chem. Eng. Sci.*, 2017, **158**, 539–544.

36 A. M. Fidelli, B. Karadeniz, A. J. Howarth, I. Huskić, L. S. Germann, I. Halasz, M. Etter, S.-Y. Moon, R. E. Dinnebier, V. Stilinović, O. K. Farha, T. Friščić and K. Užarević, Green and rapid mechanosynthesis of high-porosity NU- and UiO-type metal-organic frameworks, *Chem. Commun.*, 2018, **54**, 6999–7002.

37 D. Prochowicz, J. Nawrocki, M. Terlecki, W. Marynowski and J. Lewiński, Facile Mechanosynthesis of the Archetypal Zn-Based Metal-Organic Frameworks, *Inorg. Chem.*, 2018, **57**, 13437–13442.

38 I. Brekalo, W. Yuan, C. Mottillo, Y. Lu, Y. Zhang, J. Casaban, K. T. Holman, S. L. James, F. Duarte, P. A. Williams, K. D. M. Harris and T. Friščić, Manometric real-time studies of the mechanochemical synthesis of zeolitic imidazolate frameworks, *Chem. Sci.*, 2020, **11**, 2141–2147.

39 I. Brekalo, K. Lisac, J. R. Ramirez, P. Pongrac, A. Puškarić, S. Valić, Y. Xu, M. Ferguson, J. M. Marrett, M. Arhangelskis, T. Friščić and K. T. Holman, Mechanochemical Solid Form Screening of Zeolitic Imidazolate Frameworks Using Structure-Directing Liquid Additives, *J. Am. Chem. Soc.*, 2025, **147**, 27413–27430.

40 S.-Q. Wang, S. Darwish and M. J. Zaworotko, The impact of solution *vs.* slurry *vs.* mechanochemical syntheses upon the sorption performance of a 2D switching coordination network, *Inorg. Chem. Front.*, 2023, **10**, 3821–3827.

41 W.-Y. Gao, A. Sur, C.-H. Wang, G. R. Lorzing, A. M. Antonio, G. A. Taggart, A. A. Ezazi, N. Bhuvanesh, E. D. Bloch and D. C. Powers, Atomically Precise Crystalline Materials Based on Kinetically Inert Metal Ions *via* Reticular Mechanopolymerization, *Angew. Chem., Int. Ed.*, 2020, **59**, 10878–10883.

42 Z. Tegudeer, L. C. Davenport, M. E. Kordesch and W.-Y. Gao, Harnessing Mechanochemistry for Direct Synthesis of Imine-Based Metal–Organic Frameworks, *J. Am. Chem. Soc.*, 2025, **147**, 13522–13530.

43 F. Nouar, J. F. Eubank, T. Bousquet, L. Wojtas, M. J. Zaworotko and M. Eddaoudi, Supermolecular Building Blocks (SBBs) for the Design and Synthesis of Highly Porous Metal-Organic Frameworks, *J. Am. Chem. Soc.*, 2008, **130**, 1833–1835.

44 R. Luebke, J. F. Eubank, A. J. Cairns, Y. Belmabkhout, L. Wojtas and M. Eddaoudi, The unique rht-MOF platform, ideal for pinpointing the functionalization and $CO_2$ adsorption relationship, *Chem. Commun.*, 2012, **48**, 1455–1457.

45 D. Yuan, D. Zhao, D. Sun and H.-C. Zhou, An Isoreticular Series of Metal–Organic Frameworks with Dendritic Hexacarboxylate Ligands and Exceptionally High Gas-Uptake Capacity, *Angew. Chem., Int. Ed.*, 2010, **49**, 5357–5361.

46 D. Zhao, D. Yuan, D. Sun and H.-C. Zhou, Stabilization of Metal−Organic Frameworks with High Surface Areas by the Incorporation of Mesocavities with Microwindows, *J. Am. Chem. Soc.*, 2009, **131**, 9186–9188.

47 Y. Zou, M. Park, S. Hong and M. S. Lah, A designed metal–organic framework based on a metal–organic polyhedron, *Chem. Commun.*, 2008, 2340–2342.

48 S. Hong, M. Oh, M. Park, J. W. Yoon, J.-S. Chang and M. S. Lah, Large $H_2$ storage capacity of a new polyhedron-based metal–organic framework with high thermal and hygroscopic stability, *Chem. Commun.*, 2009, 5397–5399.

49 Y. Yan, X. Lin, S. Yang, A. J. Blake, A. Dailly, N. R. Champness, P. Hubberstey and M. Schröder, Exceptionally high $H_2$ storage by a metal–organic polyhedral framework, *Chem. Commun.*, 2009, 1025–1027.

50 W.-Y. Gao, R. Cai, T. Pham, K. A. Forrest, A. Hogan, P. Nugent, K. Williams, L. Wojtas, R. Luebke, Ł. J. Weseliński, M. J. Zaworotko, B. Space, Y.-S. Chen, M. Eddaoudi, X. Shi and S. Ma, Remote Stabilization of Copper Paddlewheel Based Molecular Building Blocks in

Metal–Organic Frameworks, *Chem. Mater.*, 2015, **27**, 2144–2151.

51 V. Guillerm, D. Kim, J. F. Eubank, R. Luebke, X. Liu, K. Adil, M. S. Lah and M. Eddaoudi, A supermolecular building approach for the design and construction of metal-organic frameworks, *Chem. Soc. Rev.*, 2014, **43**, 6141–6172.

52 H. Jiang, D. Alezi and M. Eddaoudi, A reticular chemistry guide for the design of periodic solids, *Nat. Rev. Mater.*, 2021, **6**, 466–487.

53 V. Guillerm and M. Eddaoudi, The Importance of Highly Connected Building Units in Reticular Chemistry: Thoughtful Design of Metal-Organic Frameworks, *Acc. Chem. Res.*, 2021, **54**, 3298–3312.

54 M. O'Keeffe and O. M. Yaghi, Deconstructing the crystal structures of metal-organic frameworks and related materials into their underlying nets, *Chem. Rev.*, 2012, **112**, 675–702.

55 M. Klimakow, P. Klobes, K. Rademann and F. Emmerling, Characterization of mechanochemically synthesized MOFs, *Microporous Mesoporous Mater.*, 2012, **154**, 113–118.

56 Y. Chen, H. Wu, Z. Liu, X. Sun, Q. Xia and Z. Li, Liquid-Assisted Mechanochemical Synthesis of Copper Based MOF-505 for the Separation of $CO_2$ over $CH_4$ or $N_2$, *Ind. Eng. Chem. Res.*, 2018, **57**, 703–709.

57 S. S.-Y. Chui, S. M.-F. Lo, J. P. H. Charmant, A. G. Orpen and I. D. Williams, A Chemically Functionalizable Nanoporous Material $[Cu_3(TMA)_2(H2O)_3]_n$, *Science*, 1999, **283**, 1148–1150.

58 B. Chen, M. Eddaoudi, S. T. Hyde, M. O'Keeffe and O. M. Yaghi, Interwoven metal-organic framework on a periodic minimal surface with extra-large pores, *Science*, 2001, **291**, 1021–1023.

59 B. Chen, N. W. Ockwig, A. R. Millward, D. S. Contreras and O. M. Yaghi, High $H_2$ adsorption in a microporous metal-organic framework with open metal sites, *Angew. Chem., Int. Ed.*, 2005, **44**, 4745–4749.

60 J. F. Eubank, F. Nouar, R. Luebke, A. J. Cairns, L. Wojtas, M. Alkordi, T. Bousquet, M. R. Hight, J. Eckert, J. P. Embs, P. A. Georgiev and M. Eddaoudi, On Demand: The Singular rht Net, an Ideal Blueprint for the Construction of a Metal–Organic Framework (MOF) Platform, *Angew. Chem., Int. Ed.*, 2012, **51**, 10099–10103.

61 B. Zheng, J. Bai, J. Duan, L. Wojtas and M. J. Zaworotko, Enhanced $CO_2$ binding affinity of a high-uptake rht-type metal-organic framework decorated with acylamide groups, *J. Am. Chem. Soc.*, 2011, **133**, 748–751.

62 T. Seo, N. Toyoshima, K. Kubota and H. Ito, Tackling Solubility Issues in Organic Synthesis: Solid-State Cross-Coupling of Insoluble Aryl Halides, *J. Am. Chem. Soc.*, 2021, **143**, 6165–6175.

63 N. Brown, Z. Alsudairy, R. Behera, F. Akram, K. Chen, K. Smith-Petty, B. Motley, S. Williams, W. Huang, C. Ingram and X. Li, Green mechanochemical synthesis of imine-linked covalent organic frameworks for high iodine capture, *Green Chem.*, 2023, **25**, 6287–6296.

64 H. Pan, N. Wang and G.-W. Wang, Mechanochemically synthesized covalent organic frameworks as catalysts for the Suzuki–Miyaura coupling reaction, *Chem. Commun.*, 2025, **61**, 8184–8187.

65 H. Chen, D. Feng, F. Wei, F. Guo and A. K. Cheetham, Hydrogen-Bond-Regulated Mechanochemical Synthesis of Covalent Organic Frameworks: Cocrystal Precursor Strategy for Confined Assembly, *Angew. Chem., Int. Ed.*, 2025, **64**, e202415454.

66 S. T. Emmerling, L. S. Germann, P. A. Julien, I. Moudrakovski, M. Etter, T. Friščić, R. E. Dinnebier and B. V. Lotsch, *In situ* monitoring of mechanochemical covalent organic framework formation reveals templating effect of liquid additive, *Chem*, 2021, **7**, 1639–1652.

67 G. Das, D. Balaji Shinde, S. Kandambeth, B. P. Biswal and R. Banerjee, Mechanosynthesis of imine, β-ketoenamine, and hydrogen-bonded imine-linked covalent organic frameworks using liquid-assisted grinding, *Chem. Commun.*, 2014, **50**, 12615–12618.

68 E. H. Cordes and W. P. Jencks, On the Mechanism of Schiff Base Formation and Hydrolysis, *J. Am. Chem. Soc.*, 1962, **84**, 832–837.

69 R. W. Layer, The Chemistry of Imines, *Chem. Rev.*, 1963, **63**, 489–510.

70 K. Wu, W. Zhao, L. Huang, W. T. Zeng, Q. Zhu, H. B. Wang, Q. H. Wang, X. Shi, H. Li, W. Lu, G. H. Ning, D. Zhao and D. Li, Aqueous-Phase Synthesis of Cyclic Trinuclear Cluster-Based Metal-Organic Frameworks, *J. Am. Chem. Soc.*, 2025, **147**, 13711–13720.

71 M. Ferguson, N. Giri, X. Huang, D. Apperley and S. L. James, One-pot two-step mechanochemical synthesis: ligand and complex preparation without isolating intermediates, *Green Chem.*, 2014, **16**, 1374–1382.

72 X. Li, J. Wang, F. Xue, Y. Wu, H. Xu, T. Yi and Q. Li, An Imine-Linked Metal–Organic Framework as a Reactive Oxygen Species Generator, *Angew. Chem., Int. Ed.*, 2021, **60**, 2534–2540.

73 B. Zheng, Z. Yang, J. Bai, Y. Li and S. Li, High and selective $CO_2$ capture by two mesoporous acylamide-functionalized rht-type metal–organic frameworks, *Chem. Commun.*, 2012, **48**, 7025–7027.

74 L. Rajput, D. Kim and M. S. Lah, Conformational control of ligands to create a finite metal–organic cluster and an extended metal–organic framework, *CrystEngComm*, 2013, **15**, 259–264.

75 W. Zeng, G. Wang, B. Zheng, Z. Wang and J. Bai, A porous amide-functionalized pto-type MOF exhibiting selective capture and separation of cationic MB dye, *J. Coord. Chem.*, 2021, **74**, 241–251.

76 P. Müller, R. Grünker, V. Bon, M. Pfeffermann, I. Senkovska, M. S. Weiss, X. Feng and S. Kaskel, Topological control of 3,4-connected frameworks based on the $Cu_2$-paddle-wheel node: tbo or pto, and why?, *CrystEngComm*, 2016, **18**, 8164–8171.

77 N. Zhu, M. J. Lennox, G. Tobin, L. Goodman, T. Duren and W. Schmitt, Hetero-Epitaxial Approach by Using Labile Coordination Sites to Prepare Catenated Metal-Organic Frameworks with High Surface Areas, *Chem.–Eur. J.*, 2014, **20**, 3595–3599.

78 N. Zhu, M. J. Lennox, T. Düren and W. Schmitt, Polymorphism of metal-organic frameworks: direct comparison of structures and theoretical $N_2$-uptake of topological pto- and tbo-isomers, *Chem. Commun.*, 2014, **50**, 4207–4210.

79 N. Zhu, D. Sensharma, P. Wix, M. J. Lennox, T. Düren, W. Y. Wong and W. Schmitt, Framework Isomerism: Highly Augmented Copper(II)-Paddlewheel-Based MOF with Unusual (3,4)-Net Topology, *Eur. J. Inorg. Chem.*, 2015, **2016**, 1939–1943.